Efficaciously Modeling Exterior Electrostatic Problems with Singularity for Electron Devices

Yunn-Shiuan Liao, Shiang-Woei Chyuan, and Jeng-Tzong Chen

For the performance of electron devices, an accurate electrostatic analysis is essential, and the boundary element method (BEM) has become a better method than the domain-type finite element method (FEM) because BEM can provide a complete solution in terms of boundary values only with substantial savings in modeling effort for the variable design stage. But, for exterior problems with singularity arising from the degenerate boundary (e.g., the edge of parallel-plate capacitor), the dual BEM becomes one of the most efficacious and robust tools for simulating the fringing field near the edge of electron devices because no laborious artificial boundary technique was needed like conventional BEM. After the fringing field is known well, the charge and capacitance of electron devices can be accurately calculated, and we can also understand the minimum allowable data of dielectric strength for keeping off dielectric breakdown.

Electrostatics, as used here, involves charges in motion as well as at rest. Generally, there are five fundamental quantities (voltage, charge, current, capacitance, and resistance) in electrostatics that are involved in almost all applications. For most electrical engineers, voltage, or electromotive force (EMF) is the most important one. Electrostatic problems generally play a very important role in improving the performance and reliability of electron devices in the design stage [1]. Although we all understand that the beginning of electrostatic theory is believed to have occurred several centuries before, the first meaningful application, the commercially electrostatic precipitator, was just installed by Cottrell in 1907 [2]. Besides two major present technologies from 1907 to

 8755-3996/04/$20.00 ©2004 IEEE

now, electrostatic precipitation and electrostatic coating, Castle also suggested that there would be several new industrial applications to come from developments in the fields of microelectromechanical systems (MEMS), biotechnology, ultrafine particles, nanotechnology, and space for the future applications of electrostatics [3]. Because electrostatics still affects the performance of MEMS and electron devices critically nowadays, how to accurately obtain the electric potential V and electric field intensity E becomes especially important for engineers. We all know that scientists and engineers usually use several techniques in solving continuum or field problems. Loosely speaking, these techniques can be classified as experimental, theoretical (or analytical), or numerical.

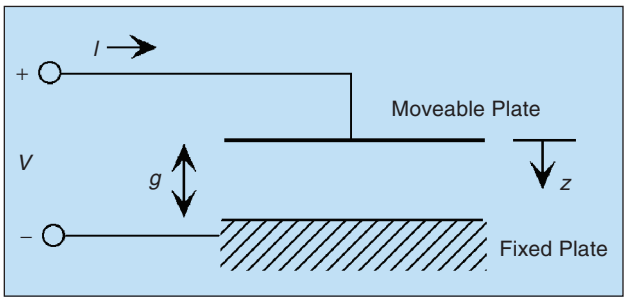

1. A parallel-plate capacitor; voltage is the across variable and current is the through variable.

USING THE EXPERIMENTAL, THEORETICAL, OR NUMERICAL METHOD TO MEET THE CASE

Among the aforementioned techniques, experimental method can measure the actual data for the finished products, but it cannot work really well in the design stage because no given goods can be used. In a word, experiments are expensive, time consuming, sometimes hazardous, and usually do not allow much flexibility in parameter variation. Therefore, designers and analysts must choose theoretical or numerical models for their needs. We all also understand that theoretical models were the first choice for researchers and scientists because of totally correct and unique solutions. Although the most satisfactory solution of a field problem is an exact mathematical one, theoretical models were scarcely utilized to predict physical response because of the very complex geometrical designs and loading transfer paths in pragmatic design problems. In reality, an analytical solution to an electrostatic problem has only been possible for certain simple configurations and material properties, which are represented by relatively simple models.

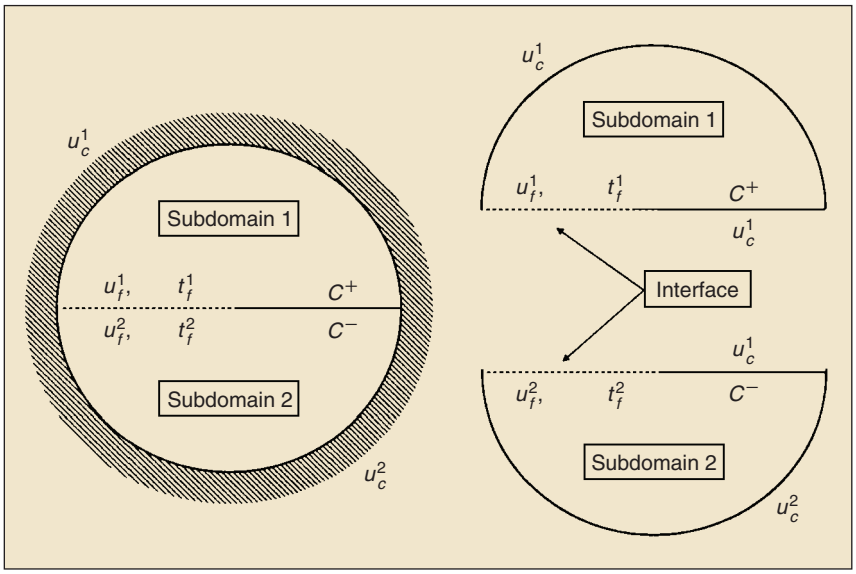

2. A figure sketch of the multidomain.

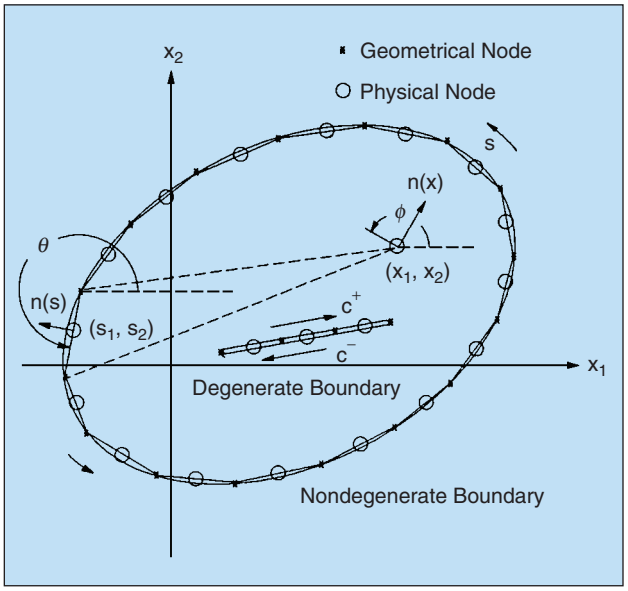

3. Boundary element discretization for degenerate boundary and nondegenerate boundary.

For example, the development of solid-state microwave devices and systems has led to the widespread use of a form of parallel-plate transmission lines called microstrip lines or, simply, striplines. Because the analytical results were based on the assumption of two wide conducting plates (with negligible fringing effect) of equal width, they are not expected to apply exactly for variable designs. The analytical approximation is closer only if the width of the metal strip is much greater than the substrate thickness, because not all the fields will be confined in the dielectric substrate: some will stray from the top strip into the region outside of the strip, thus causing interference in the neighboring circuits. As we see, an exact analytical solution of the above-mentioned stripline satisfying all the boundary conditions is difficult or nearly impossible, so efficient numerical methods have to be used for the more complex electron devices. So, our problem concerns what kind of numerical method is valuable to recommend for researchers and engineers in the field of electrostatics?

REVIEW AND COMPARISON OF BEM AND FEM

Before recommending a robust method, let's review diverse computational techniques in electromagnetics (EM). From scientific history, we find that most EM problems were solved using the classical methods of separation of variables and integral equation solutions until the 1940s. Computational solution of electrical problems started in the mid-1960s with the availability of modern high-speed digital computers. Since then, scientists have expended effort on solving practical, complex EM-related problems for which closed-form analytical solutions are either intractable or not available. The numerical approach has the advantage of allowing the actual work to be carried out by operators without knowledge of higher mathematics or physics, with a resulting economy of labor on the part of the highly trained personnel. However, every numerical method [e.g., finite difference method (FDM), moment methods (MoM), FEM, BEM, transmission-line-matrix method (TLM), Monte Carlo method (MCM), etc.] used in EM, involves an analytical simplification to the point where it is easy to apply the numerical method [4]. Among diverse numerical approaches, the FEM and BEM have today moved from being research tools for select groups to become powerful design tools for engineers, and those two numerical methods have been regularly used in MEMS and EM.

As we see, the FEM, based on the representation and approximate solution of boundary value problems of engineering mathematics in terms of partial differential equations [5], and the BEM, based on the integral equation, have moved from being research tools for scientists to powerful design tools for engineers [6]. One of the main advantages of BEM, when compared to FEM, is that discretizations are restricted only to the boundaries, making data generation much easier. The BEM is also ideally suited to the analysis of external problems where domains extend to infinity, since discretizations are confined to the internal boundaries with no need to truncate the domain at a finite distance and impose artificial boundary conditions and to problems involving some form of discontinuity or singularity due to the use of singular fundamental solutions as test functions. It is also interesting to point out that the unknowns in the BEM are a mixture of the potential and its normal derivative, rather than the potential only, as in FEM. This is a consequence of the BEM being a "mixed" formulation and constitutes an important advantage over the FEM. Especially for the design of electron devices (e.g., variable gaps between upper movable and lower fixed plates of parallel-plate capacitors), many laborious works of finite element modeling compared with those of boundary element model are needed because BEM can provide a complete solution in terms of boundary values only, with substantial saving in modeling effort. Therefore, there is no doubt that BEM has been become a very appealing approach in numerical simulation of MEMS and EM [7], even if many of today's engineers still use commercial packages and waste much time to set up adverse FEM models in the design stage. Following the review and comparison of diverse numerical

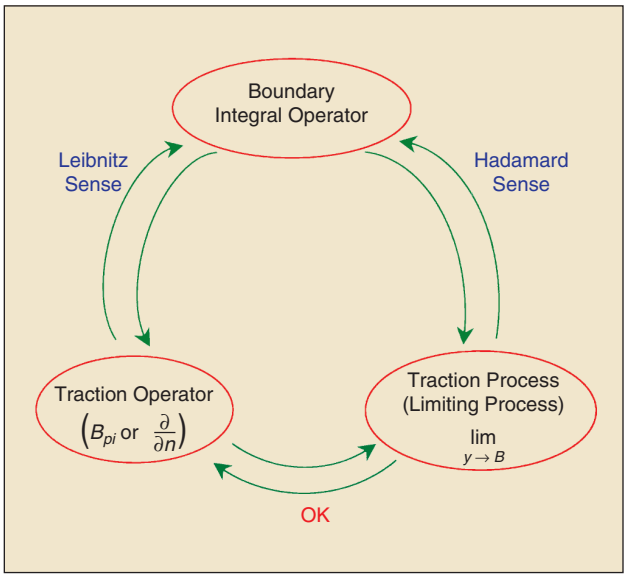

4. Commutativity of trace and differential operator.

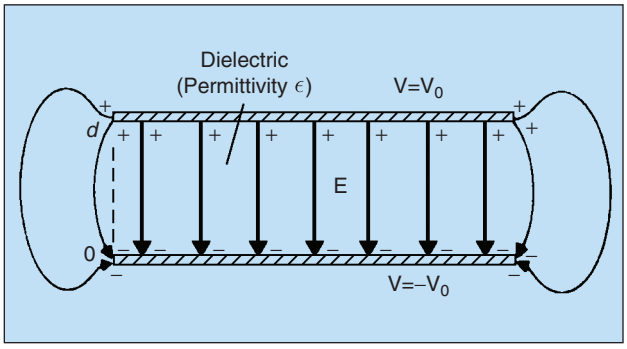

5. Cross section and electric intensity field of a parallel-plate capacitor.

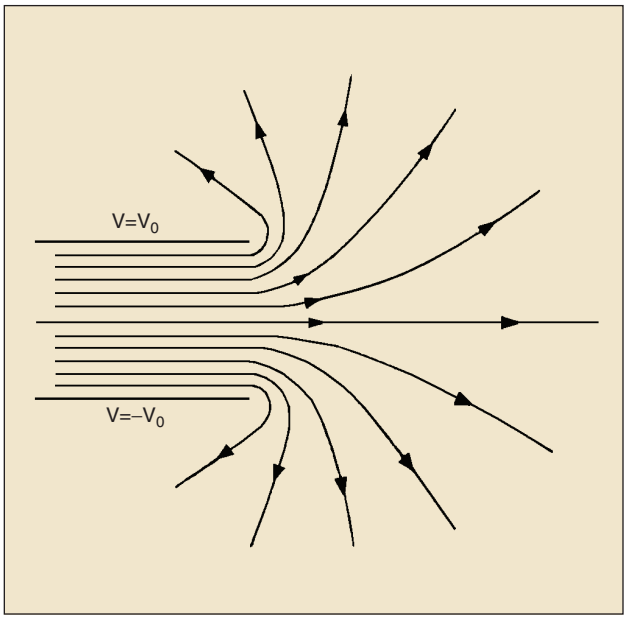

6. Electric potential field near the edge of a parallel-plate capacitor.

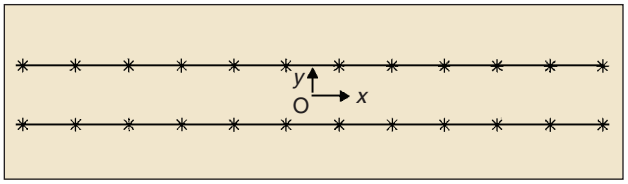

7. The related DBEM mesh discretization of the parallel-plate capacitor.

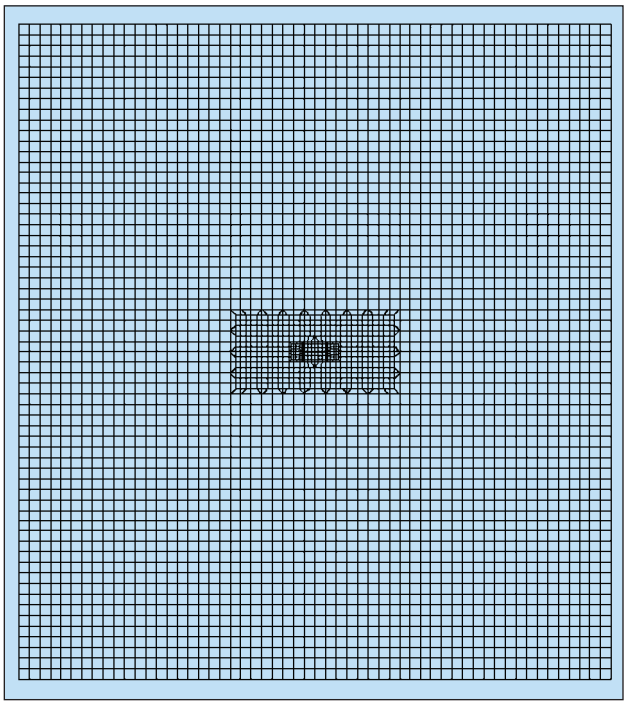

8. The related FEM mesh discretization of the parallel-plate capacitor.

techniques, we will explain the reason for using the dual BEM (DBEM) to take the place of the conventional BEM in the following section.

WHY USE DBEM FOR EXTERIOR ELECTROSTATIC PROBLEMS WITH SINGULARITY?

We all have known the suitability and superiority of BEM for infinite field, but a more powerful method—DBEM will be introduced in this article. Why? Because modern electron device design usually contains very thin conducting plates for MEMS and electron devices (e.g., a parallel-plate capacitor shown in Figure 1), we will face the numerical singularity arising from the degenerate boundary (The degenerate boundary refers to a boundary, two portions of which approach each other such that the exterior region between the two portions becomes infinitely thin.) if using conventional BEM to simulate the fringing effect around the edge of electrostatic devices, and the coincidence of the boundaries gives rise to an ill-conditioned problem. In order to model this singularity and to ensure a unique solution, we will use the inconvenient subtechnique for degenerate boundary using the conventional BEM. If the concerned domain was divided into different subdomains with artificial boundaries, new interfaces between subdomains are formed. (Since the unknown pairs of $\{u_f^1\}$, $\{u_f^2\}$, $\{t_f^1\}$ and $\{t_f^2\}$ are introduced in the artificial boundary as shown in Figure 2, two constraints of the continuity and equilibrium conditions: $\{u_f^1\} = \{u_f^2\}$ and $\{t_f^1\} = -\{t_f^2\}$, where u_f is the potential and t_f is the normal derivative along the interface boundary.) Because some new unknowns are introduced in the artificial boundaries, new constraints of the continuity and equilibrium conditions are necessary. But the main drawback of the technique is that the deployment of artificial boundaries is arbitrary and, thus, cannot be implemented easily into an automatic procedure. In addition, model creation is more troublesome than in the single-domain approach. Therefore, we urgently need to search for another efficient method to overcome this difficulty for exterior electrostatic problem with singularity.

In 1999, Chen et. al. proposed the dual integral formulations to successfully tackle such degenerate boundary problems [8]. Using the dual integral formulations, all the above-mentioned boundary value problems can be solved efficiently in the original single domain, and the fringing effect can be modeled very well. That is why we recommend DBEM to analyze the exterior electrostatic problems with singularity caused by a degenerate boundary. We have understood the

Table 1. The results of electric potential of the parallel-plate capacitor under diverse numerical methods.

Locations (x, y)	$V(x, y)$ from conventional BEM without artificial boundary	$V(x, y)$ from DBEM	$V(x,y)$ from FEM	Difference
(30.00, 20.00)	N/A	$0.11737V_0$	$0.120966V_0$	–2.973%
(25.00, 15.00)	N/A	$0.13914V_0$	$0.1444641V_0$	–3.685%
(20.00, 10.00)	N/A	$0.17050V_0$	$0.1787659V_0$	–4.624%
(15.00, 4.50)	N/A	$0.20792V_0$	$0.2255798V_0$	–4.268%
(10.00, 4.00)	N/A	$0.52458V_0$	$0.5171448V_0$	–1.438%
(6.667, 7.00)	N/A	$0.58679V_0$	$0.6054016V_0$	–3.074%
(3.333, 4.00)	N/A	$0.81123V_0$	$0.8197266V_0$	–4.122%
(0.00, 7.00)	N/A	$0.67831V_0$	$0.6879212V_0$	–1.037%
(0.00, 4.00)	N/A	$0.82767V_0$	$0.8330323V_0$	–1.679%
(0.00, 10.00)	N/A	$0.56037V_0$	$0.5717102V_0$	–0.644%
(30.00, 5.00)	N/A	$0.044234V_0$	$0.046167V_0$	–4.187%
(25.00, 5.00)	N/A	$0.066191V_0$	$0.06957398V_0$	–4.862%

suitability of DBEM over conventional BEM while facing singularity. A brief introduction of DBEM will be introduced in the following section.

BACKGROUND OF DBEM FOR EXTERIOR ELECTROSTATIC PROBLEMS

For a homogeneous medium, we know that the governing equation of electrostatics can be written in the following form:

$$\nabla^2 V = -\rho/\varepsilon, \tag{1}$$

where ∇^2 is the *Laplacian* operator. *Poisson's* equation (1) states that the divergence of the gradient of electric potential V equals $-\rho/\varepsilon$ for a simple medium, where ε is the permittivity of the medium and ρ is the volume density of free charges. At points in a simple medium where there is no free charge, (1) is reduced to

$$\nabla^2 V = 0, \tag{2}$$

also known as *Laplace's* equation, which plays a very important role in MEMS and EM. It is the governing equation for electrostatic problems involving a set of conductors, such as capacitors, maintained at different potentials. Once V is found from (2), E can be determined from $-\nabla V$, and the charge distribution on the conductor surfaces can be determined from surface-charge density $\rho_s = \varepsilon E_n$, because the normal component of the electric field at a conductor boundary is equal to the surface charge density on the conductor divided by the permittivity [1].

The electrostatic problem consists of finding the unknown potential function Φ (or V) in the partial differential equation. In addition to the fact that Φ satisfies (2) within a prescribed solution region Ω, the potential function Φ must satisfy certain conditions on B, which is the boundary of Ω. Usually, these boundary conditions are the Dirichlet and Neumann types. Therefore, the governing equation and boundary conditions of electrostatic problems could be written in the following form.

- *Governing equation:*

$$\nabla^2 \Phi(x) = 0, \quad x \text{ in } \Omega \tag{3}$$

- *Dirichlet boundary condition:*

$$\Phi(x) = f(x), \quad x \text{ on } B \tag{4}$$

9. The results of electric potential field (equipotential lines) of the parallel- plate capacitor using DBEM (red: $+V_0$; blue: $-V_0$).

10. The results of electric potential field (equipotential lines) of the parallel-plate capacitor using FEM (red: $+V_0$; blue: $-V_0$).

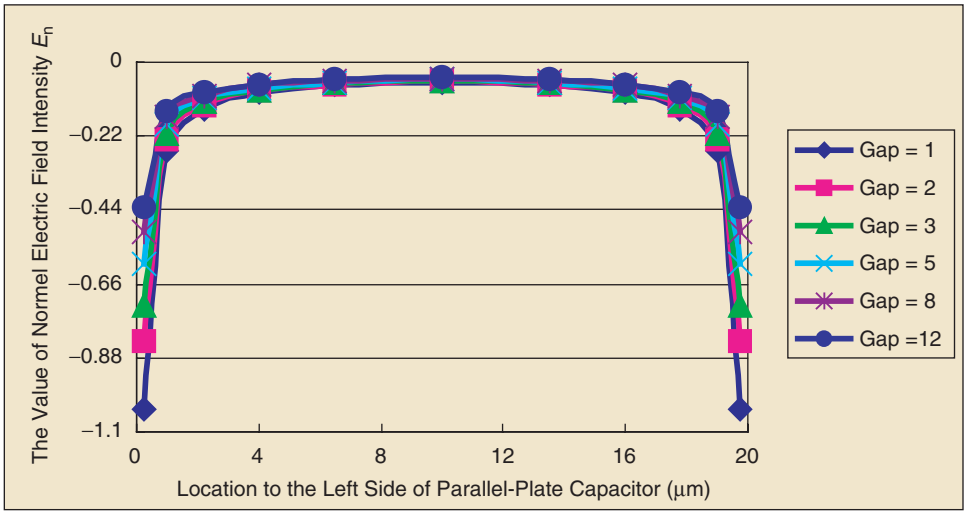

11. The distribution of normal electric field intensity (E_n) on the top side of upper movable plate under diverse gaps design. (unit: $V_0/\mu m$).

✦ *Neumann boundary condition:*

$$\partial\Phi(x)/\partial n_x = g(x), \quad x \text{ on } B \tag{5}$$

where $f(x)$ and $g(x)$ denote the known boundary data, and n_x is the unit outer normal vector at the point x on the boundary.

Based on the dual boundary integral equation formulation [8], we have

$$\alpha\Phi(x) = \text{CPV}\int_B T(s,x)\Phi(s)\,\mathrm{d}B(s) - \text{RPV}\int_B U(s,x)[\partial\Phi(s)/\partial n_s]\,\mathrm{d}B(s) \tag{6}$$

$$\alpha[\partial\Phi(x)/\partial n_x] = \text{HPV}\int_B M(s,x)\Phi(s)\mathrm{d}B(s) - \text{CPV}\int_B L(s,x)[\partial\Phi(s)/\partial n_s]\mathrm{d}B(s), \tag{7}$$

where the kernel functions, $U(s,x) = \ln(r)$, $T(s,x) = \partial U(s,x)/\partial n_s$, $L(s,x) = \partial U(s,x)/\partial n_x$, $M(s,x) = \partial^2 U(s,x)/\partial n_x \partial n_s$, $r = |s-x|$, s and x being position vectors of the points s and x, respectively, and n_s is the unit outer normal vector at point s on the boundary (see Figure 3). In addition, RPV is the Riemann principal value, CPV is the Cauchy principal value, HPV is the Hadamard principal value, and α depends on the collocation point ($\alpha = 2\pi$ for an interior point, $\alpha = \pi$ for a smooth boundary, and $\alpha = 0$ for an exterior point). The commutativity property of the trace operator and the normal derivative operator provides us with alternative ways to calculate the HPV analytically [8]. First, L'Hospital's rule is employed in the limiting process. Second, the normal derivative of the CPV should be taken carefully by using Leibnitz' rule, and then the finite part can be obtained. The finite part has been termed the HPV or Mangler's principal value. In the derivation of dual equations, two alternatives can be applied to determine the HPV as shown in Figure 4. Generally, (6) is called the *singular boundary integral equation*, and (7) is called the *hypersingular boundary integral equation*.

The linear algebraic equations for an electrostatic problem discretized from the dual boundary integral equations can be written as

$$\left[T^i_{pq}\right]\{\Phi_q\} = [U_{pq}]\{\partial\Phi/\partial n\}_q \tag{8}$$

$$\left[M^i_{pq}\right]\{\Phi_q\} = [L_{pq}]\{\partial\Phi/\partial n\}_q \tag{9}$$

where $\{\Phi_q\}$ and $\{\partial\Phi/\partial n\}_q$ are the boundary potential and flux, and the subscripts p and q correspond to the labels of the collocation point and integration element, respectively. The influence coefficients of the four square matrices $[U]$, $[T]$, $[L]$ and $[M]$ for interior exterior problem can be represented as

$$U^i_{pq} = \text{RPV}\int_{Bq} U(s_q, x_p)\,\mathrm{d}B(s_q) \tag{10}$$

$$T^i_{pq} = -\pi\delta_{pq} + \text{CPV}\int_{Bq} T(s_q, x_p)\,\mathrm{d}B(s_q) \tag{11}$$

$$L^i_{pq} = \pi\delta_{pq} + \text{CPV}\int_{Bq} L(s_q, x_p)\,\mathrm{d}B(s_q) \tag{12}$$

$$M^i_{pq} = \text{HPV}\int_{Bq} M(s_q, x_p)\,\mathrm{d}B(s_q), \tag{13}$$

where B_q denotes the qth element and $\delta_{pq} = 1$ if $p = q$, otherwise it is zero. Based on the matrix relations between the interior and exterior electrostatic problems, the technique for the interior problem can be easily reintegrated. According to the dependence of the out-normal vectors in these four kernel functions for the interior and exterior electrostatic problems, their relationship can be easily found:

$$U^i_{pq} = U^e_{pq} \tag{14}$$

$$M^i_{pq} = M^e_{pq} \tag{15}$$

$$T^i_{pq} = -T^e_{pq} \quad \text{if } p \neq q\,;\; T^i_{pq} = T^e_{pq} \quad \text{if } p = q \tag{16}$$

$$L^i_{pq} = -L^e_{pq} \quad \text{if } p \neq q\,;\; L^i_{pq} = L^e_{pq} \quad \text{if } p = q. \tag{17}$$

CASE STUDY: HOW DBEM WORKS FOR PARALLEL-PLATE CAPACITORS?

In order to demonstrate the suitability and efficiency of DBEM for solving the singularity arising from degenerate boundaries, let's use a typical parallel-plate capacitor. Basically, for the nondegenerate boundary problems, either conventional BEM [just using the first kind kernels of $U(s,x)$ and $T(s,x)$ or the second kind kernels of $L(s,x)$, $M(s,x)$] or DBEM [using the first kind kernels of $U(s,x)$, $T(s,x)$ and the second kind kernels of $L(s,x)$, $M(s,x)$ in the meantime] can be used. But for the exterior electrostatic problems with degenerate boundaries, as in the following case, DBEM plays an important role, but conventional BEM without artificial boundaries cannot be used.

Case Study

A parallel-plate capacitor consists of two parallel conducting plates of length l separated by a uniform distance (or gap) d, and two parallel plates maintained at potentials V_0 and $-V_0$ for upper movable and lower fixed plates that form a parallel-plate capacitor, as shown in Figure 5. Determine the electrostatic field near the edge (see Figure 6). Because the gap d between movable and fixed plates can play a very important role for the capacitance C and charge Q of parallel-plate capacitors, also investigate the effect of variable d.

FEM Analysis

From Figures 5 and 6, as we see that there is an obvious fringing effect near the edge of the capacitor, and the physical behavior (e.g., electric potential and electric field intensity) of this area is very complex. Therefore, the approximate results [1] in which based on the assumption of two wide conducting plates (with negligible fringing effect) could not be used to simulate

the local response near the edge of the capacitor. Because it is not easy to obtain the accurate solutions just using analytical methods, the FEM simulation [9] was used to compare with the following DBEM data. Due to exterior fields, a huge finite-element model must be set up to satisfy the infinite prescribed boundary condition and to obtain a reasonable result.

DBEM Analysis

For convenience, the length l and distance d of our parallel-plate capacitor are assumed to be 20 and 2 μm separately, and 12 points will be analyzed using rough mesh discretization (44 elements and 24 nodes, see Figure 7) of DBEM and compared with reference data computed from a huge FEM model (3,976 elements and 12,120 nodes, see Figure 8). Because many FEM models need to be established for diverse gap variation, FEM is not a good choice for variable gaps between these two metal plates, so we use DBEM to perform the following tasks since the discretizations of DBEM are restricted only to the boundaries, making data generation much easier than FEM. The results of electric potential by way of conventional BEM without artificial boundaries, DBEM, and FEM were listed in Table 1 and shown in Figures 9 and 10. Comparing the results of electric potential field (equipotential lines) using DBEM (see Figure 9) and FEM (see Figure 10), we can see that the difference of electric potential distribution is very little. Because fringing field action also affects device parameters (e.g., the threshold voltage, an important design parameter, depends upon the channel width and thick field oxide extent [10]), The DBEM used in this article is a very efficiently numerical method for the exterior electrostatic problems with singularity.

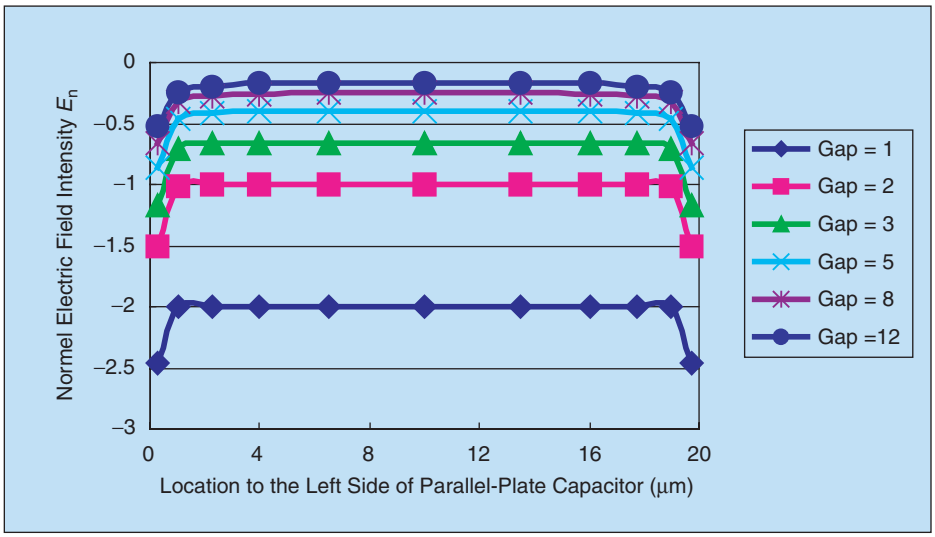

12. The distribution of normal electric field intensity (E_n) on the bottom side of upper movable plate under diverse gaps design. (unit: $V_0/\mu m$).

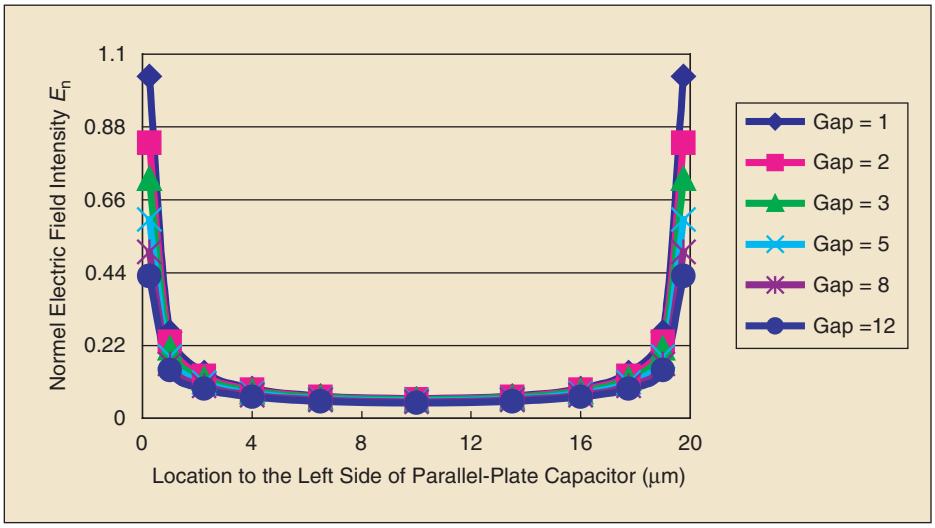

13. The distribution of normal electric field intensity (E_n) on the bottom side of lower fixed plate under diverse gaps design. (unit: $V_0/\mu m$).

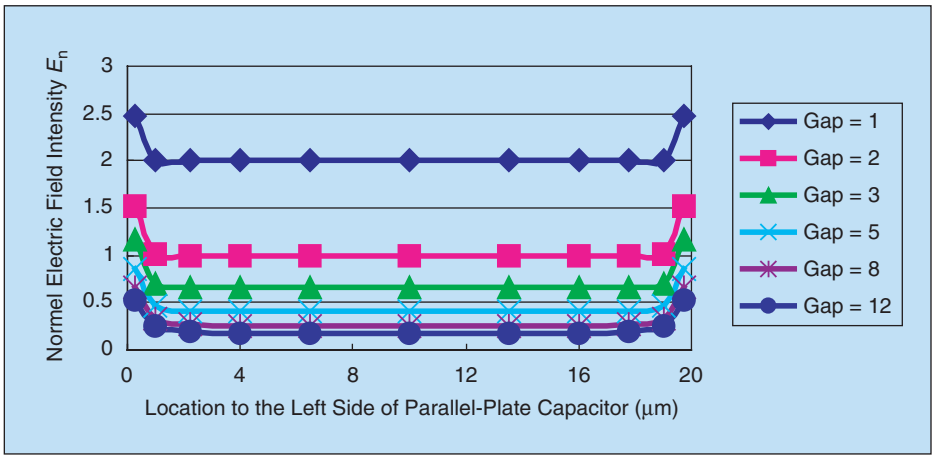

14. The distribution of normal electric field intensity (E_n) on the top side of lower fixed plate under diverse gaps design. (unit: $V_0/\mu m$).

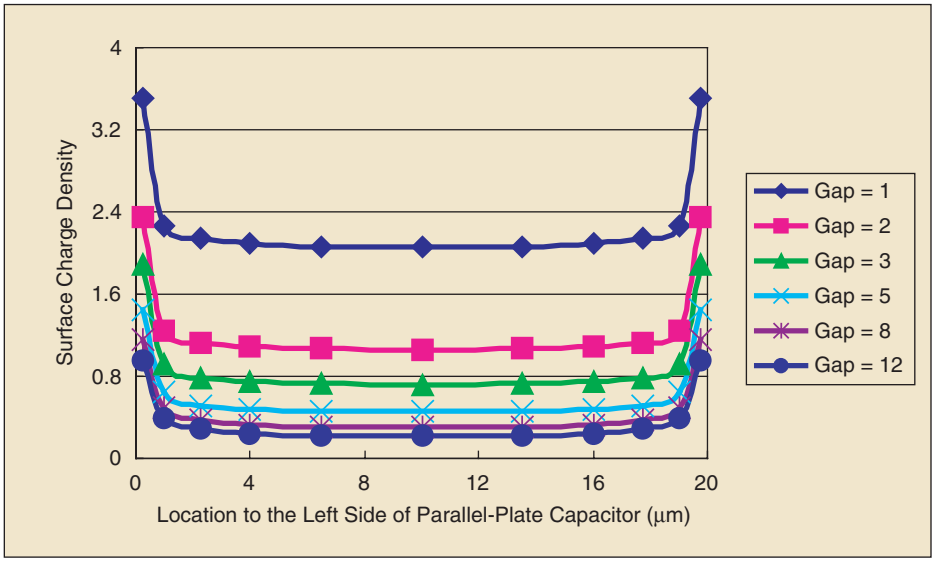

15. The distribution of surface charge density (ρ_s) of upper movable plate under diverse gaps design. (unit: $\varepsilon V_0/\mu m^2$).

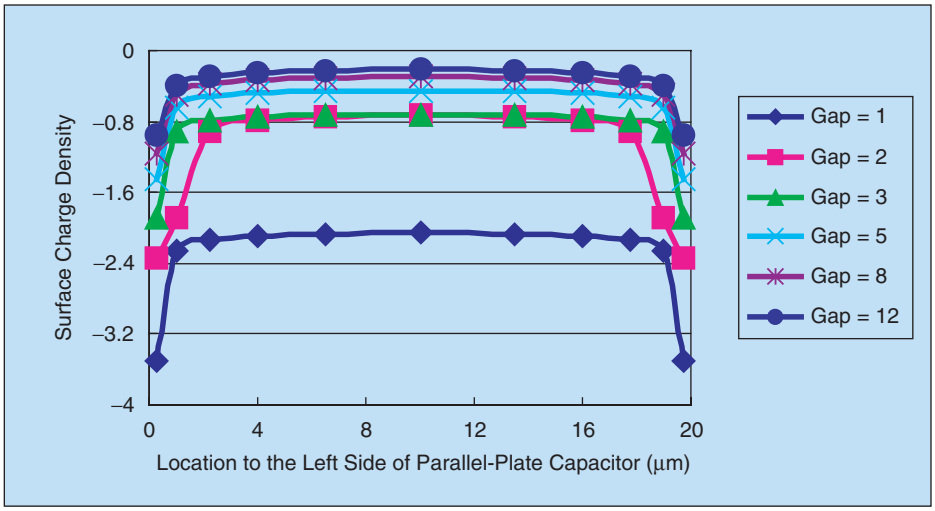

16. The distribution of surface charge density (ρ_s) of lower fixed plate under diverse gaps design. (unit: $\varepsilon V_0/\mu m^2$).

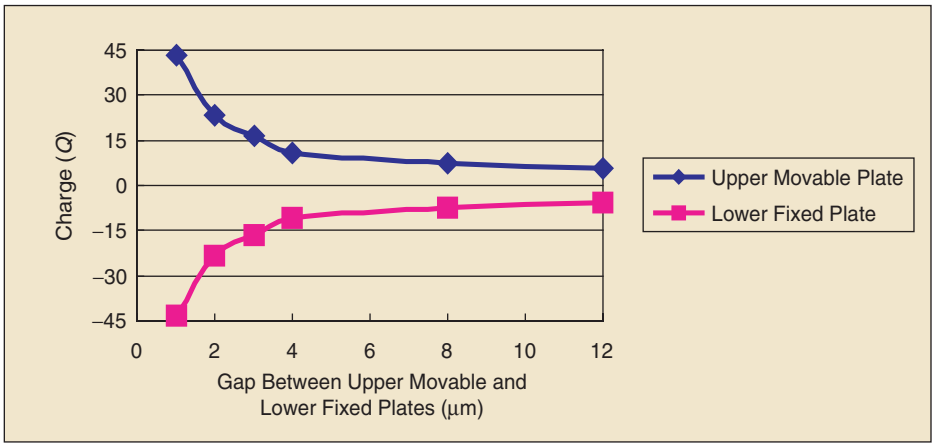

17. The distribution of charge (Q) on both upper movable and lower fixed plates under diverse gaps design. (unit: $\varepsilon w V_0$).

By way of DBEM, the distribution of normal electric field intensity E_n on the bottom and top sides of the upper movable plate under diverse values of d were shown in Figures 11 and 12, respectively. From Figures 11 and 12, we can see that the values of E_n on the bottom side of the upper movable plate are obviously dependent on the values of d and the location to the left corner of metal plate loc_x, but the E_n on the top side are only obviously dependent on loc_x not d. Similarly, the distribution of E_n on the bottom and top sides of the lower fixed plate under diverse values of d were shown in Figures 13 and 14, respectively. From Figures 13 and 14, we also can see that the values of E_n on the top side of the lower fixed plate are still obviously dependent on the values of d and loc_x, but the E_n on the bottom side are only obviously dependent on loc_x, not d. From Figures 11–14, we make that the following interesing observations:

- ✦ The values of E_n on the edge of parallel-plate capacitor are much higher than those on the middle part because of fringing effect.
- ✦ The smaller the d is, the larger the E_n is.

THE EFFECT OF GAP VARIATION FOR CHARGE AND CAPACITANCE DISTRIBUTION

As we know, the value of d can play a very important role; let's investigate the effect of gap variation between upper movable and lower fixed plates for charge and capacitance distribution. Because the charge distribution on the conductor surfaces can be determined from $\rho_s = \varepsilon E_n$ (The normal component of the electric field E_n at a conductor boundary is equal to the surface charge

density ρ_s on the conductor divided by the permittivity ε [1]) if ε is a constant. From Figures 15 and 16, we can see that the values of surface charge density ρ_s on both the upper movable and lower fixed plates are obviously dependent on the values of d and loc_x. We know that the fringing effect around the edge of parallel-plate capacitors is as clear as day, like E_n. From these results, we can see the ρ_s at the edges becomes much larger than that at the center for parallel-plate capacitors because of fringing effect. If the width of parallel-plate capacitors is w, the distribution of charge Q on both upper movable and lower fixed plates under diverse gaps design can be shown in Figure 17, where we can see that the smaller the value of d is, the larger the Q of the parallel-plate capacitor is.

Furthermore, we hope understand the relationship between capacitance C of the parallel-plate capacitor and the values of d. Let's start this with a typical two-conductor capacitor first, which consists of two conductors separated by free space or a dielectric medium. The conductors may be of arbitrary shapes, as shown in Figure 18. When a dc voltage source is connected between the conductors, a charge transfer occurs, resulting in a charge $+Q$ one conductor and $-Q$ on the other. The value of C ($C = Q/V_{12}$, where V_{12} is the difference of voltage between these two conductors) of a capacitor is a physical property of the two-conductor system and depends on the geometry of the conductors and on the permittivity of the medium between them [1], [11]. If the fringing effect around the edge of parallel-plate capacitor (see Figure 5) is ignored for simplification, the analytical value of C for our parallel-plate capacitor is $20\,\varepsilon w/d$ ($=\varepsilon\, lw/d$). By way of DBEM, we can accurate the above-mentioned fringing effect to obtain the distribution of ρ_s and Q for the parallel-plate capacitor under diverse d. Therefore, the numerical value of C for our parallel-plate capacitor considering the fringing effect can be shown in Figure 19, and the smaller the value of d is, the larger the C of parallel-plate capacitors is. By the way, the increase of charge at the edges is due to fringing action and gives rise to fringing capacitances, because the effect of fringing at the edges of conductors can be seen directly from the distribution of charge on surfaces of conductors having edges. Furthermore, we also can find the comparison of capacitance between DBEM considering the fringing effect and analytical method neglecting the fringing effect under diverse gap from Figure 20, where the larger the value of d is, the larger the difference between these methods is. Therefore, the influence of fringing effect around the edge of parallel-plate capacitor becomes more significant as the value d of becomes larger.

> We strongly recommend our DBEM for future variable design of electron devices since they can save a lot of cost and time.

Finally, we can summarize that

- ✦ Conventional BEM without artificial boundaries cannot solve the exterior electrostatic problem with degenerate boundaries like the edge of parallel-plate capacitors. DBEM can analyze the exterior electrostatic problem with degenerate boundary very efficiency, but the first kind kernels of $U(s, x)$, $T(s, x)$ and the second kind kernels of $L(s, x)$, $M(s, x)$ need to be used simultaneously.
- ✦ In estimating C of parallel-plate capacitors considering the fringing field around the edge of conductors, DBEM is very useful primarily because, in the approach, one solves directly for the surface charges in the conductors.

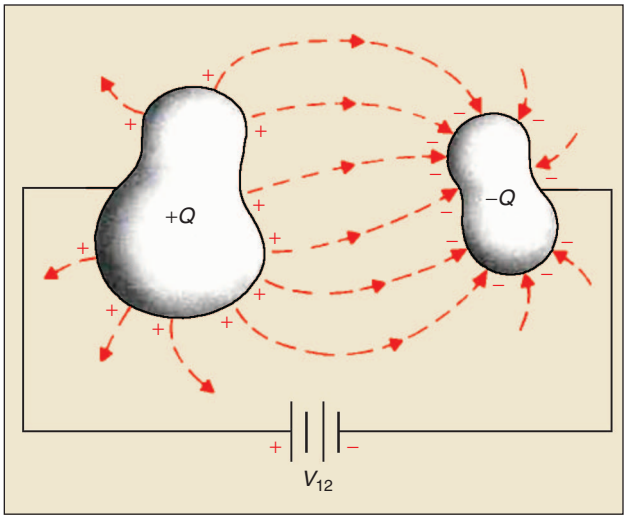

18. A typical two-conductor capacitor.

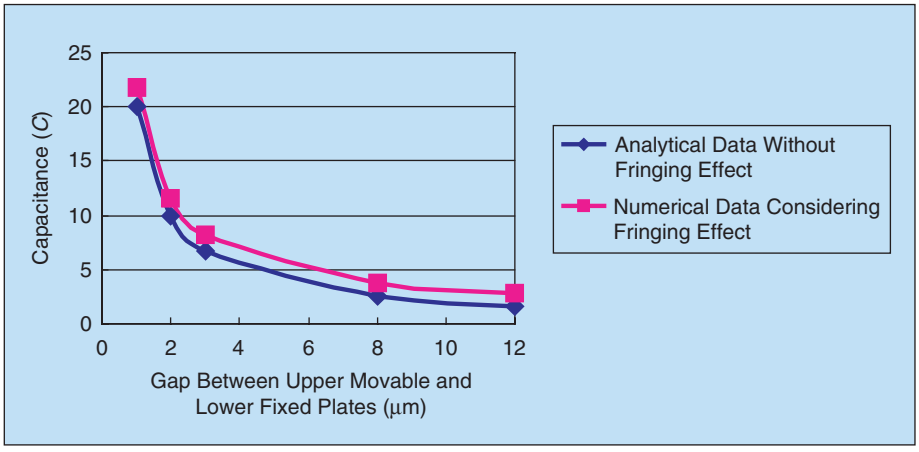

19. The distribution of capacitance (C) of the parallel-plate capacitor under diverse gaps design (unit: εw).

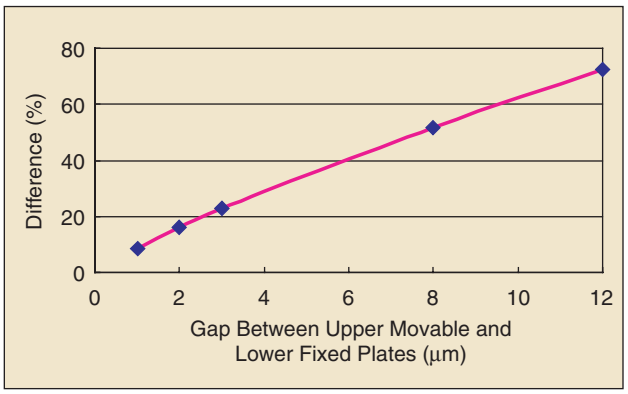

20. The difference of capacitance C of parallel-plate capacitor between DBEM and analytical data.

- The values of E_n on both the movable and lower fixed plates are all obviously dependent on the values of d and loc_x. We know that the fringing effect around the edge of parallel-plate capacitors is apparent.
- The values of ρ_s on both the upper movable and lower fixed plates are also obviously dependent on the values of d and loc_x. We also can see the ρ_s at the edges becomes much larger than that at the center for parallel-plate capacitors because of fringing effect. The smaller the value of d is, the larger the Q of parallel-plate capacitors is.
- The smaller the value of d is, the larger the C of parallel-plate capacitors is. The increase of charge at the edges of the parallel-plate capacitor is due to fringing action and gives rise to fringing capacitances.
- The larger the value of d is, the larger the difference between these methods is, and the influence of fringing effect around the edge of parallel-plate capacitor becomes more significant as the value d of becomes larger.

CONCLUSION AND RECOMMENDATION

As we know from the theory of electrostatics [1], the electric field will cause small displacements of the bound charges in a dielectric material, resulting in polarization. If the electric field is very strong, it will pull electrons completely out of the molecules. The electrons will accelerate under the influence of the electric field, collide violently with the molecular lattice structure, and cause permanent dislocations and damage in the material. Then, the avalanche effect of ionization due to collisions may occur, and the material will become conducting, and large currents may result. This phenomenon is called a dielectric breakdown, and the maximum electric field intensity that a dielectric material can withstand without breakdown is the dielectric strength of the material. So the accurate and efficient modeling for fringing effect around the edge of electron devices is very important for performance because we need to know the minimum allowable data of dielectric strength for keeping off dielectric breakdown. Therefore, the DBEM presented in this article is an efficient tool for exterior electrostatic problems with singularity arising from degenerate boundary.

In basic electrostatics, the formula for the capacitance of parallel-plate capacitors is derived for the case that the spacing between the electrodes is very small compared to the length or width of the plates. However, when the separation is wide, the formula for very small separation does not provide accurate results because no fringing effect is considered (e.g., unequal plates design [12]). Although many researchers have successfully used BEM for diverse applications in the field of EM and MEMS [13]–[15], they still need use the indirect skill of artificial boundaries while facing the singularity. For electrical engineering practices, since the major effort is model creation, the DBEM—a more direct and easier method, free from the development of an artificial boundary, has great potential for industrial applications. Therefore, we strongly recommend our DBEM for future variable design of electron devices since they can save a lot of cost and time.

Yunn-Shiuan Liao and *Shiang-Woei Chyuan* are with National Taiwan University, Taipei, Taiwan, ROC. *Jeng-Tzong Chen* is with National Taiwan Ocean University, Keelung, Taiwan, ROC. E-mail: yeaing@iris.seed.net.tw.

REFERENCES

[1] D.K. Cheng, *Field and Wave Elctromagnetics*. Reading, MA: Addison-Wesley, 1989.

[2] H.J. White, "Centenary of Frederick Gardner Cottrell," *J. Electrostat.*, vol. 4, pp. 1–34, Dec. 1997.

[3] G.S.P. Castle, "Industrial applications of electrostatics: The past, present and future," *J. Electrostat.*, vol. 51–52, pp. 1–7, May 2001.

[4] M.N.O. Sadiku, *Numerical Techniques in Electromagnetics*. Boca Raton, FL: CRC, 1992.

[5] J. Jin, *The Finite Element Method in Electromagnetics*. New York: Wiley, 2002.

[6] M.H. Aliabadi, *The Boundary Element Method*. New York: Wiley, 2002.

[7] Y.S. Liao, S.W. Chyuan, and J.T. Chen, "An alternatively efficient method (DBEM) for simulating the electrostatic field and levitating force of a MEMS combdrive," *J. Micromech. Microeng.*, vol. 14, pp. 1258–1269, Aug. 2004.

[8] J.T. Chen and H.K. Hong, "Review of dual boundary element methods with emphasis on hypersingular integrals and divergent series," *Trans. ASME, J. Appl. Mech.*, vol. 52, no. 1, pp. 17–33, 1999.

[9] *I-DEAS User's Guide, Finite Element Modelin.*, SDRC, 1990.

[10] D.N. Pattanayak, J.G. Poksheva, R.W. Downing, and L.A. Akers, "Fringing field effect in MOS devices," *IEEE Trans. Comp. Hybrids. Manufact. Technol.*, vol. 5, pp. 127–131, Mar. 1982.

[11] H. Nishiyama and M. Nakamura, "Form and capacitance of parallel-plate capacitors," *IEEE Trans. Comp. Packag. Manufact. Technol. A*, vol. 17, pp. 477–484, Sept. 1994.

[12] W. Lin, "Computation of the parallel-plate capacitor with symmetrically placed unequal plates," *IEEE Trans. Microwave Theory Tech.*, vol. 33, pp. 800–807, Sept. 1985.

[13] J. Wiersig, "Boundary element method for resonances in dielectric microcavities," *J. Opt. A: Pure Appl. Opt.*, vol. 5, pp. 53–60, Jan. 2003.

[14] W. Ye, S. Mukherjee, and N.C. MacDonald, "Optimal shape design of an electrostatic comb drive in microelectromechanical systems," *IEEE J. Microelectromech. Syst.*, vol. 7, pp. 16–26, Feb. 1998.

[15] S. Chakravorti and H. Steinbigler, "Boundary element studies on insulator shape and electric field around HV insulators with or without pollution," *IEEE Trans. Dielect. Elect. Insulation*, vol. 7, pp. 167–176, Apr. 2000. CD ■